ADVANCES IN FLOW BOILING HEAT TRANSFER AND ITS RELEVANCE FOR ENERGY SYSTEMS DESIGN

F. MAYINGER

Lehrstuhl A für Thermodynamik
Technische Universität München
Munich / Germany

ABSTRACT

In spite of more than 30 years research there are still open questions for the design of equipment in power and process industries working under flow boiling heat transfer. Especially areas where major thermal non-equilibrium exists, like under subcooled boiling or post dry-out conditions, superheating of the continuous two-phase flow, behaviour of the dispersed phase, transport phenomena and void fraction are of interest.

Measurements with sophisticated instrumentation brought new insights into the mechanism of nucleation, bubble-growth and -recondensation and allow to formulate better correlations for predicting void fraction and pressure drop with subcooled boiling.

In the post dry-out region the cooling of the wall is strongly influenced by the distribution of the droplet swarm versus the cross section of the channel and by the superheating of the vapour. The local concentration of the droplets is of main interest in bends, where centrifugal forces- pressure gradients and secondary flow cause a varying distribution of the droplets along the way through the bend. Measurements proved that the average heat transfer under post dry-out conditions is higher in bends than in straight tubes. Due to the secondary flow, rewetting can occur not only at the outer, but also at the inner part of the bend.

1. PARTICULARITIES OF TWO-PHASE FLOW

Two-phase flow in power cycles usually is composed of a liquid substance - mostly water - and its vapour forming a mixture of various flow pattern. The rate of the vapour flow in the mixture is called quality

$$\dot{x} = \frac{\dot{m}_V}{\dot{m}_V + \dot{m}_L} = \frac{\dot{m}_V}{\dot{m}} \tag{1}$$

and with increasing vapour mass flow the phases start to separate and form an annular configuration with a liquid film at the wall and a vapour core in the centre of the channel having droplets embedded. The droplet swarm is called entrainment. At low qualities bubbly flow exists and flow pattern between bubbly flow and annular flow are slug flow and churm flow. At high qualities the liquid film at the wall becomes completely entrained either by evaporation due to heat addition or by friction forces from the vapour flow. Then spray- or fog-flow can be observed.

Vapour and liquid do not flow with the same velocity and, therefore, the local volumetric vapour content - called void fraction -

$$\epsilon = \frac{V_V}{V_V + V_L} = \frac{A_V}{A_V + A_L} \tag{2}$$

and by this the portion of the cross-section of the channel taken by the vapour cannot be simply calculated by using the density ratios of vapour and liquid to convert the quality into the void fraction. Using the velocity ratio s, called slip

$$s = \frac{w_V}{w_L} \tag{3}$$

of the phases the connection between quality and void fraction is given by

$$\frac{\epsilon}{1-\epsilon} = \frac{\dot{x}}{1-\dot{x}} \cdot \frac{\varrho_L}{\varrho_V} \cdot \frac{1}{s} \tag{4}$$

Components of plants in the power- and process-industries in which evaporation and two-phase flow exists are boilers, pre-heaters, the core of water cooled nuclear reactors, but also the low pressure stages of steam turbines.

In all these components phase change occurs due to energy transport or with enthalphy change resulting from increasing or decreasing kinetic energy. A correct and reliable design of these components needs information on phase change phenomena and mainly on the effect of boiling.

In a fossil boiler, for example, liquid being not yet at saturation condition enters the tube, the liquid is heated up starts to evaporate first under nucleate boiling and later on when the void fraction is increasing under surface boiling and finally the heat emitting wall becomes dry and superheated vapour is produced still having embedded small droplets of saturated liquid.

In the entrance region of the boiler tube evaporation at the heated wall starts already at a position where the bulk of the liquid is still subcooled, i.e. its temperature is below the saturation temperature. The reason is that due to heat addition from the wall there is a temperature gradient in the boundary layer and the temperature of the liquid in immediate neighbourhood of the wall may be already above the saturation temperature. Bubble formation and by this nucleate boiling does not start exactly when the liquid reaches saturation temperature. Depending on the surface tension of the liquid and the roughness of the wall a certain thermodynamic dis-equilibrium is needed for starting and driving the nucleation process. On the other side the vapour bubbles growing in the superheated boundary layer begin to condense again when they reach the subcooled bulk of the liquid flow. This situation - called subcooled boiling - implies various conditions of thermal dis-equilibrium.

Another area of thermal dis-equilibrium can be found at the down-stream end of the boiler tube, when most of the liquid is evaporated and the wall is not wetted. The heat emitted from the wall is superheating the vapour and this superheated vapour gives part of his heat to the liquid droplet swarm still existing in the flow. The droplets are slowly evaporating by this heat addition from the superheated vapour. In bends these droplets tend to flow to the outer radius of the bend due to centrifugal forces. This produces an additional dis-equilibrium, because now the droplet concentration and by this the cooling ability is higher at the outer radius of the bend than at the inner one.

2. SUBCOOLED BOILING

2.1 Onset of Subcooled Boiling

Neglecting the effects of subcooled boiling can lead to a sizing of a boiler far away from real physical conditions. As mentioned before with high heat fluxes vapour bubbles are produced at the tube walls in spite of the fact that the mean liquid temperature - averaged over the cross-section - is below the saturation temperature. The position and by this the subcooling at which nucleation and bubble formation starts is a function of the heat flux, the mass flow

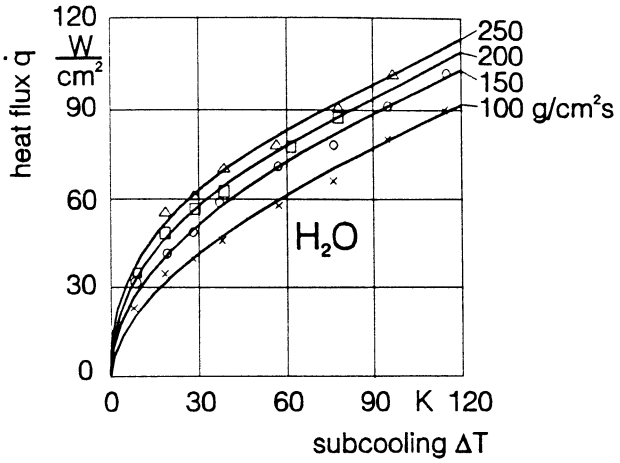

Figure 1: Onset of subcooled boiling in a rod bundle (Water, 100 bar)

rate and the physical properties of the substance, like surface tension, specific heat, thermal conductivity and latent heat of evaporation. There are several papers in the literature dealing with subcooled boiling /3,9,15,19,20,22,23/. Fig. 1 gives a global impression on the correlation between heat flux and local subcooling at which bubble formation starts. The data presented there /15/ were measured in water at a pressure of 100 bar.

Intending to find a more general law for the onset of subcooled nucleate boiling the author performed experiments with a modelling liquid - the refrigerant R12 - and compared the results with data from the literature investigated in water and in other substances. To formulate a correlation for calculating the onset of nucleate boiling as function of thermal and hydrodynamic parameters an empirical exponential equation of the following type was chosen.

$$Bo = C Re^{a} \left(\frac{p}{p_{crit}}\right)^{b} Ja_{mod}^{c} \tag{5}$$

The boiling number

$$Bo = \frac{q_{onb}}{\dot{m}\Delta h_{VL}} \tag{6}$$

represents the ratio of total heat flux emitted by the wall versus the energy which is transported in the fluid from the wall by latent heat of evaporation. The Reynolds-number

$$Re = \frac{\dot{m} D_h}{\eta} \tag{7}$$

takes in account the velocity profile of the flow in the tube. The reduced pressure (p/p_{crit}) is used as a scaling parameter for fluid-fluid modelling assuming a similar behaviour of all substances at the critical point according to the theorem of corresponding states. Finally the degree of subcooling is expressed in a modified Jacob-number

$$Ja_{mod} = \frac{h_s - h_b}{\Delta h_v} \frac{\varrho_L - \varrho_V}{\varrho_V} \tag{8}$$

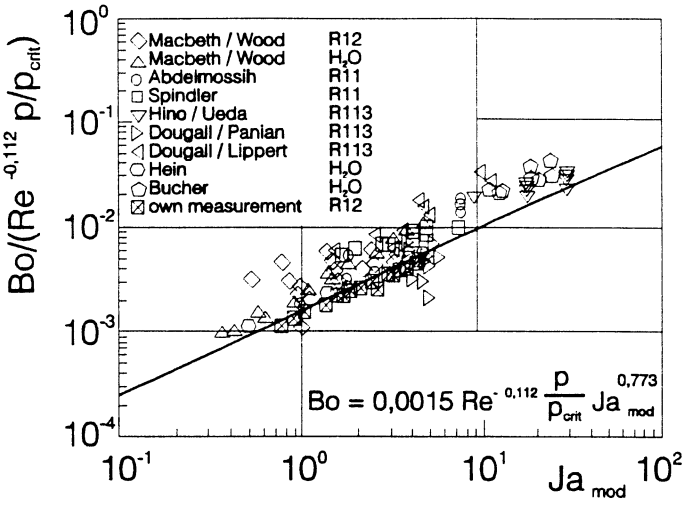

Figure 2: Onset of nucleate boiling for various substances (Comparison: experimental data with equ. 5a)

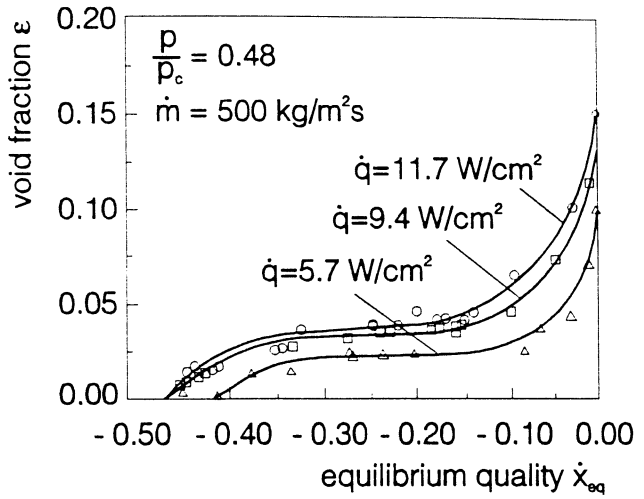

Figure 3: Development of void fraction with equilibrium quality at subcooled boiling (Refrig. R12)

To determine the constant C and the exponents in equ.5a stepwise multiple regression analysis was used. The result of this regression analysis is summarised in equ.5a.

$$Bo = 0.0015\ Re^{-0.112}\ \frac{p}{p_{crit}}\ Ja_{mod}^{0.773} \qquad (5\ a)$$

In a first consideration it is astonishing that the exponent on the Reynolds-number in equ.5a is negative and, as a result, the mass flow rate also has a negative exponent. Taking into account the fact that the mass flux is included in the denominator of the boiling number also, the resultant exponent on the mass flux will be 0,89 and this value is in good agreement with the correlations from the literature for heat transfer with single-phase flow.

Fig.2 shows how equ.5a based on the own experimental data agrees with measured data in the literature /1,5,6,11,12,14,16,17,21,/ taking in account also experiments in water.

2.2 Void Fraction

In the experiments /4/ also the void fraction near the position of onset of subcooled boiling was measured using an impedance void meter. In fig.3 the volumetric void fraction under the conditions of subcooled boiling is plotted versus the equilibrium quality defined by

$$x_{eq} = \frac{h_L - h_{SL}}{h_{LV}} \simeq \frac{c_p\,(T(z) - T_s)}{h_{LV}} \qquad (9)$$

where $T(z)$ is the mean bulk temperature (according to Dix /10/) at the axial position z. The data shown in this figure were measured at the same reduced pressure $p/p_c = 0,48$ and the same mass flux $\dot{m} = 500$ kg/m^{2}s. The inlet subcooling has been varied from 10 to 50 K. Analysing the data, void fraction under the conditions of subcooled bulk flow has a first increase at the early beginning of the vapour formation. Then the void fraction stays nearly constant over a wide range of equilibrium quality until a point of significant vapour generation. A similar observation was made by Bjorge /2/. This behaviour can be explained by the fluiddynamic situation in the tube. At very high subcooling the bubbles remain attached to the wall and recondense at the position they grew, in the very thin superheated liquid layer. The slip ratio (equ.3) is smaller than 1 because the liquid flows faster than the bubbles mostly resting at the wall. So even a very small amount of vapour takes a relative large part of the cross-section of the channel. With decreasing subcooling the bubbles can grow larger, because recondensation becomes smaller and they are now able to detach from the heated surface. They can slide along the wall and flow into the bulk where they finally condense. The slip ratio tends to 1 now and finally becomes larger than 1 which means that the bubbles start to travel faster than the liquid resulting in a phase separation. A reason for the almost constant void fraction in this zone (see fig.3) in spite of increased evaporation is the increasing slip ratio (see equ.4). Finally the vapour production exceeds the recondensation rate. The void is now increasing exponentially.

The influence of the mass flow rate on the onset of subcooled boiling and on the behaviour of the void fraction mediates fig.4. In this figure three different mass flux densities are plotted together gaged at the same pressure and heat flux density. The void fraction decreases with increasing mass flux as to be expected. The arrow placed at the x_{eq}- axes indicates the calculated onset of nucleate boiling using equ.5a for the mass flux of $\dot{m} = 2500$ kg/m^{2}s.

An example of the radial void profile measured with gamma ray attenuation and of the radial temperature distribution in the fluid is given in fig.5 for a mass flux density of 1500 kg/m^{2}s, and a reduced pressure of 0,48. The heat flux density from the wall to the refrigerant R12 was 7,5 W/cm^2. For equilibrium two-phase flow, i.e. with saturated conditions of vapour and liquid, the relationship

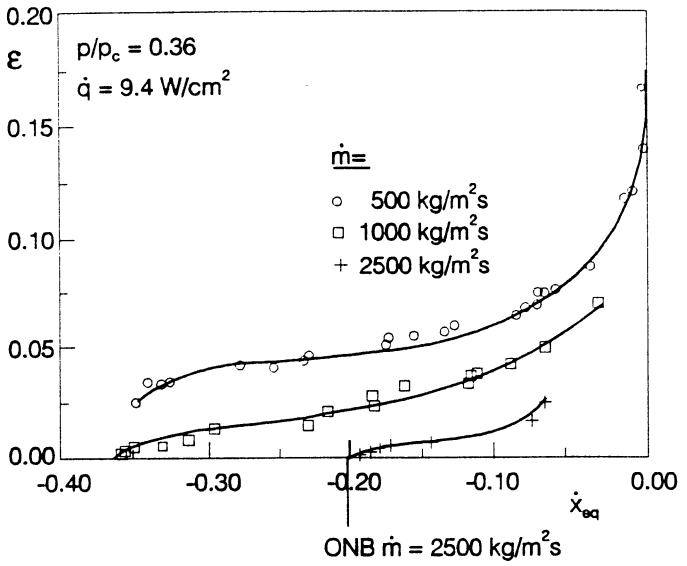

Figure 4: Influence of mass flux on void fraction with subcooled boiling (Refrig. R12)

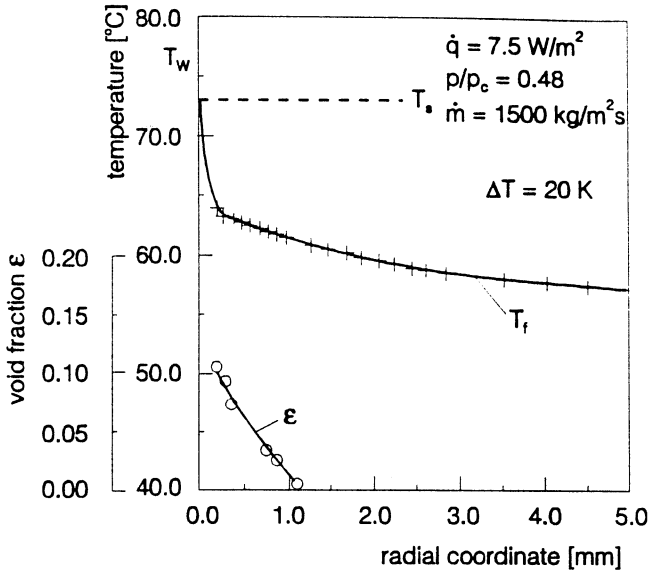

Figure 5: Radial profile of temperature and void fraction in an annulus with subcooled boiling (Refrig. R12)

between local void fraction ϵ and flow quality $\dot{x}$ is described in the literature by the drift flux model for example /27/. For obvious reasons this model should work for non-equilibrium situations - for example for subcooled boiling - also if the true flow quality $\dot{x}$ is known. This true quality is defined by

$$\dot{x} = \frac{\dot{m}_V}{\dot{m}} \tag{10}$$

with the total mass flow $\dot{m}$ and the vapour mass flow $\dot{m}_V$. This true vapour quality can be calculated by using an energy and a momentum balance. For calculating the energy balance the measurements of the temperature profile (see for example fig. 5) can be used, adding a correction proposed by Staub /24/. In the drift flux model the relationship between the local volumetric void fraction ϵ and the true flow quality $\dot{x}$ is given by

$$\epsilon = \frac{\dot{x}/\varrho_V}{C_0\ [\dot{x}/\varrho_V + (1-\dot{x})/\varrho_L] + V_{jg}/\dot{m}} \tag{11}$$

Where V_{jg} is the vapour drift velocity and C_0 the distribution coefficient. The drift velocity V_{jg} can be set to

$$V_{jg} = 1.18\ \left[\frac{\sigma\ g\ (\varrho_L - \varrho_V)}{\varrho_L^2}\right]^{0.25} \tag{12}$$

with the surface tension σ and the gravity acceleration g. Using a stepwise regression analysis of own measured data and also data published by Friedel /13/ the distribution parameter C_0 was fit to

$$C_0 = \dot{\epsilon}\left[1 + 1.049\ Fr^{-0.05}(1-Ja)^{0.164}\cdot \cdot \left(\frac{\varrho_V}{\varrho_L}\right)^{0.694}\left(\frac{1-\dot{x}}{\dot{x}}\right)\left(1-\frac{p}{p_c}\right)^{0.124}\right] \tag{13}$$

with the average volumetric flow concentration ϵ defined by

$$\dot{\epsilon} = \frac{1}{1 + \frac{1-\dot{x}}{\dot{x}}\frac{\varrho_V}{\varrho_L}} \tag{14}$$

The Froude number in equ.13 is defined by the total mass flux $\dot{m}$ and by the equivalent diameter d_{hy} as usual in the literature.

$$Fr = \frac{\dot{m}^2}{g\ d_{hy}\ \varrho_L^2} \tag{15}$$

To take in account the degree of subcooling, i.e. the inlet subcooling of the fluid, the Jacob-number

$$Ja = \frac{h_{SL} - h_{in}}{\Delta h_{LV}} \tag{16}$$

was also introduced in equ.13. Fig.6 gives an idea how the results calculated by the equations 11-16 agree with the measured data. The symbols represent the measured data the lines give the calculated behaviour.

2.3 Pressure Drop

It is to be expected that the void in the flow is considerably influencing the pressure drop with subcooled boiling. Two-phase pressure drop is usually presented in the literature in terms of the Martinelli parameter Φ^2, which is also called two-phase flow multiplier. Referred to single-phase flow it gives the factor by which the pressure drop of a two-phase mixture is higher than that of single phase flow. In fig.7 this two-phase multiplier is referred to the liquid flow and one can deduce from this figure that the void of subcooled boiling is considerably influencing the pressure drop even at high subcoolings at the inlet of the channel. Comparing fig.7 with fig.3 one finds out that the pressure drop behaves quite analogous to the void formation in the channel.

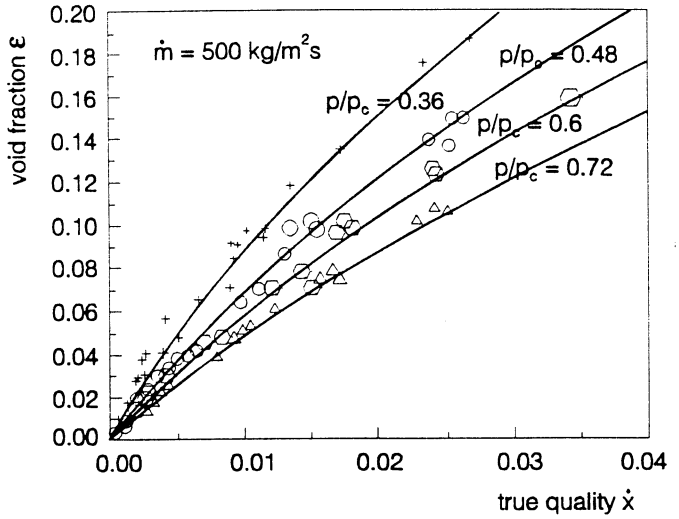

Figure 6: Comparison of predicted (equ. 10-14) and measured data for void fraction with subcooled boiling (Refrig. R12)

2.4 Recondensation of Bubbles

To develop a more sophisticated model for predicting the void fraction with subcooled boiling the heat transfer between the bubbles and the subcooled liquid has to be known. There are several publications in the literature dealing with the condensation velocity of vapour in subcooled liquid. Recently also the local and temporal heat transfer coefficient at the phase-interface of bubbles emerged in a subcooled liquid and moving there slowly was measured by using an optical method, the holographic interferometry /7,8,18/. The temporal course of the collaps of a vapour bubble during condensation in a subcooled liquid can be controlled by two different phenomena:

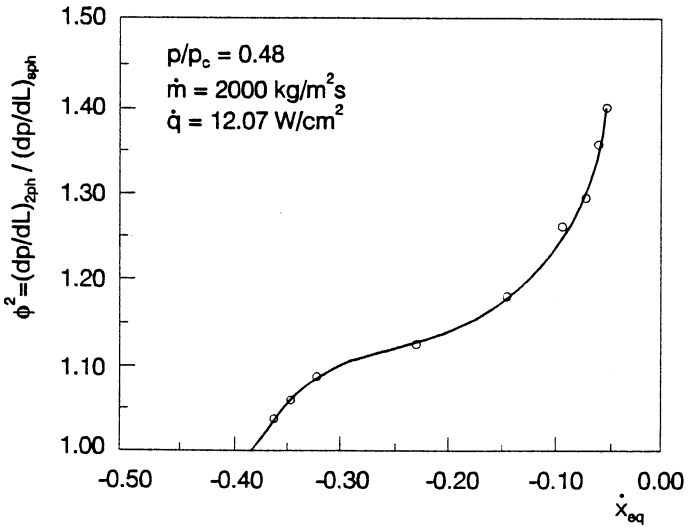

Figure 7: Pressure drop (Martinelli multiplier) with subcooled boiling (Refrig. R12)

- the heat transfer at the phase-interface of vapour and liquid and
- the inertia of the liquid mass when entering into the space set free by the condensing vapour.

With moderate temperature differences between vapour and subcooled liquid the heat transport will be the governing process for the volumetric decrease of the bubble. This heat transfer process at the phase-interface is influenced by the thermo-physical properties like heat conductivity, specific heat, latent heat of evaporation, density, viscosity and surface tension. Also the gradient of the saturation line plays a role. The thermophysical properties can be expressed in dimensionless numbers like the Prandtl-number

$$Pr = \frac{\eta_L \, c_p}{\lambda_L} \tag{17}$$

the Jacob-number defined in a little different way than equ.16

$$Ja = \frac{\varrho_L \, c_p \, (T_S - T_\infty)}{\varrho_V \, \Delta h_{LV}} \tag{18}$$

and the Reynolds-number which takes in account the moving velocity of the bubble in the liquid.

$$Re = \frac{2R \, w \, \varrho_L}{\eta_L} \tag{19}$$

Finally the Fourier-number

$$Fo = \frac{a_L \, t}{(2R)^2} \tag{20}$$

can be used as a dimensionless time for describing the duration of the collapsing period.

An example of the temporal and local course of the heat transfer at the phase-interface of a steam bubble condensing in subcooled water shows fig.8.
In this example the collaps of the bubble was completely controlled by heat transfer. The border between heat transfer- and inertia-controlled condensation can be expressed by the Jacob-number. At Jacob-numbers above 70 usually and at Jacob-numbers above 100 always inertia-controlled condensation was observed. The measurements were performed with various substances like water, ethanol, propanol and the refrigerant R113.

The results can be expressed in terms of the Reynolds- and the Prandtl-number. One has to distinguish, however, between situations when the bubble is fixed at the mouth of a nozzle with the liquid flowing over the bubble, and another situation when the bubble can freely move in the liquid. In both cases the Reynolds-number is defined by the relative velocity between bubble and liquid. For the hydraulic length in the Reynolds-number the bubble diameter is used at the beginning of the condensation. The physical properties in the Reynolds- and in the Prandtl-number are referred to the liquid phase.

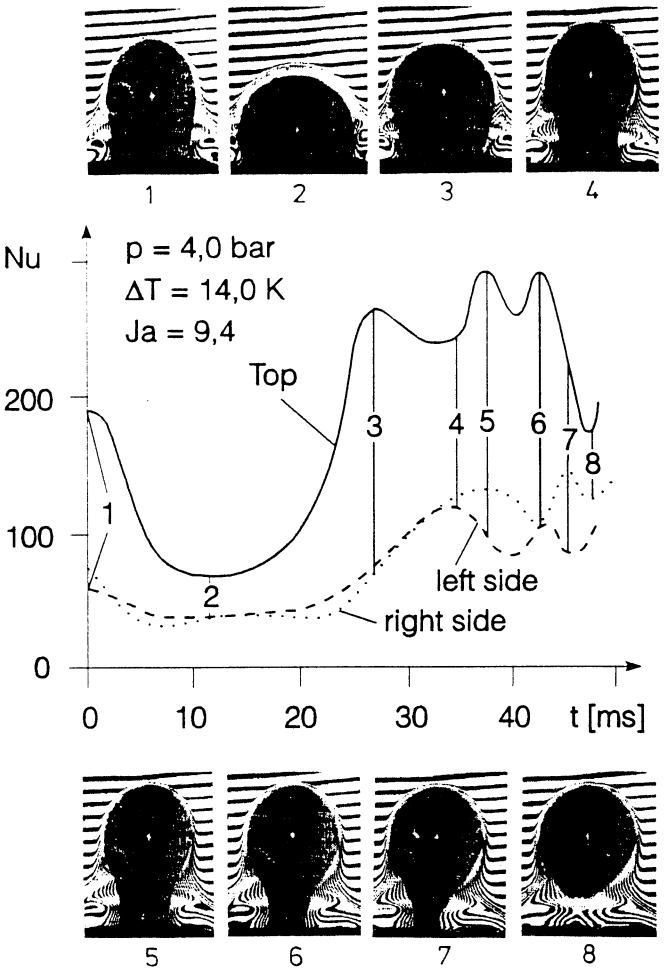

Figure 8: Heat transfer around a condensing steam bubble in subcooled water, originating from a nozzle.

For bubbles attached to a nozzle equ.21 was found by evaluating the measured data gained by the holographic interferometry.

$$Nu = 0.185\ Re^{0.7}\ Pr^{0.5} \tag{21}$$

The heat transfer at the phase-interface of moving bubbles can be expressed quite similarly

$$Nu = 0.6\ Re^{0,6}\ Pr^{0,5} \tag{22}$$

If the bubbles originate from a nozzle where saturated vapour is blown out the detachment diameter of such bubbles can easily be calculated by using equ.23

$$d = \sqrt[3]{\frac{6\ \sigma\ d_{D\ddot{u}}}{\Delta\varrho\ g}} \tag{23}$$

in which $d_{D\ddot{u}}$ represents the diameter of the nozzle mouth and g the gravity acceleration. $\Delta\varrho$ represents the density difference between the vapour and the liquid.

A comparison between experimental data measured by the holographic interferometry and the predictions of equ.21 is shown in fig.9. The heat transfer at the surface of a bubble sticking at a nozzle but exposed to a slow cross-flow is higher than that around a solid sphere which

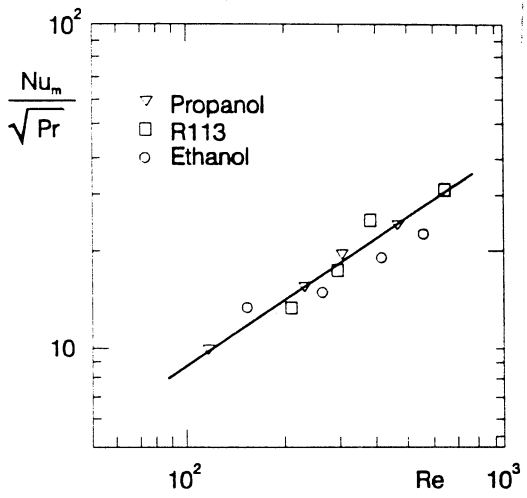

Figure 9: Average heat transfer at the phase interface of fixed vapour bubbles condensing in a subcooled liquid of the same substance. (Comparison of measured data by holographic interfereometry and equ. 21)

can be explained by the smaller shear stress at the phase-interface and by the movability of the bubble surface.

The agreement between measured data and the prediction by equ.22 is good for moving bubbles also. As shown in fig.10, equ.22 corresponds well not only for water, but also for various organic substances with measured data.

Using high-speed cinematography one gets also information about the temporal decrease of the bubble diameter which is closely related with the heat transfer at the phase interface. The duration of the bubble life can be expressed by the Fourier-number (equ.20) and using the experimental data the simple correlation

$$Fo = 1.784\ Re^{-0.7}\ Pr^{-0.5}\ Ja^{-1.0} \tag{24}$$

for predicting the total condensation period was found. Up to a Jacob-number of 70 this equation corresponds well with measured data as fig.11 shows.

Finally the temporal decrease of the bubble diameter

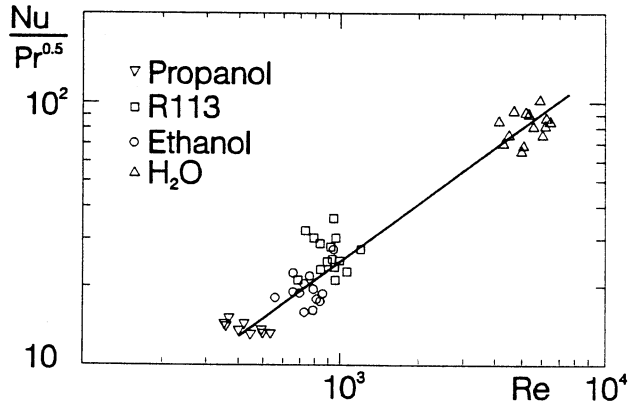

Figure 10: Average heat transfer at the phase interface of rising vapour bubbles condensing in a subcooled liquid of the same substance. (Comparison of measured data and equ. 22)

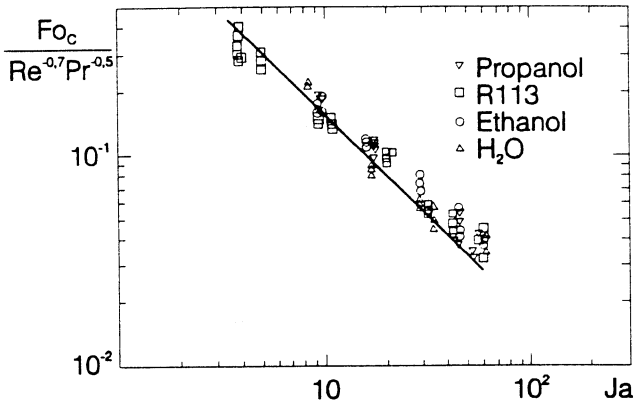

Figure 11: Length of time for bubble condensation in subcooled liquid. (Comparison of measured data with equ. 24)

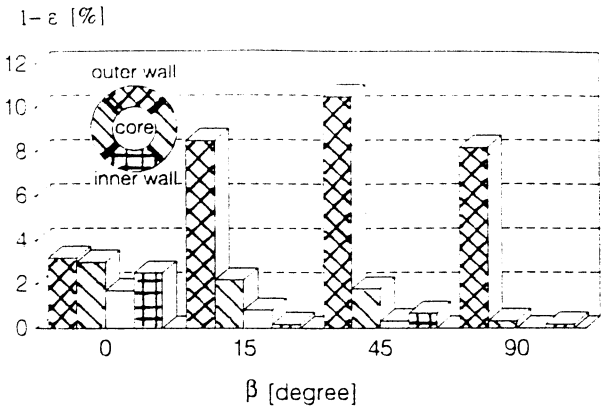

Figure 12: Phase distribution in a bend with no wall wetting. (R_{bend}/R_{tube} = 42, Refrig. R12, p= 9,5 bar. $\dot{m}$ = 680 kg/m^{2}s, $\dot{q}_W$ = 50 kW/m^2, $\dot{x}_{eq,in}$ = 0,86)

can be predicted by using equ.25.

$$\beta = \left[1 - 0.56\ Re^{0.7}\ Pr^{0.5}\ Ja\ Fo\ \right]^{0.9} \qquad (25)$$

in which β represents the ratio between the momentary diameter of the bubble during the course of condensation and the diameter when the condensation started.

3. POST-DRY-OUT DISPERSED FLOW IN CURVED CHANNELS

The droplet distribution in curved channels under post dry- out condition was recently studied by Wang and Mayinger /25,26/. An impedance probe was used to measure the local concentration of the droplets versus the cross-section and along the axis of the bend. In each cross-section the impedance probe allowed to distinguish five different measuring regions, namely an outer region that is close to the outer wall of the bend, an inner region close to the inner wall, a core region in the centre part of the tube, and two side regions. Detailed flow information at the bend inlet was obtained from a post dry-out heat transfer model developed by Wang /26/.

Fig.12 shows a typical phase-distribution which occurred at small to intermediate mass flow rates and intermediate to high heat fluxes. Wall temperature readings indicate that film boiling pattern is maintained in such conditions. As seen from the figure a significant non-symmetric flow structrue is developed in the bend. Phase separation due to the centrifugal forces brings most part of the liquid to the outer wall region, producing a liquid deficiency in inner parts of the cross-section. This process appears already at the inlet location then strengthens in the first part of the bend and reaches a maximum at about 45-deg. bend angle.

In the latter stage of the bend, from about 45-deg. bend angle on, a decrease of liquid concentration is found at the outer wall region. This is attributed partially to the evaporation process and partially to the droplet inward reversal. Due to the droplet inward motion a slight increase of liquid concentration in the inner wall region is observed. The inward motion of the droplet is produced by a secondary flow which is a consequence of the centrifugal forces and the pressure drop over the cross-section resulting from this centrifugal forces. Due to the centrifugal force the heavier component - the droplets - move outward in the low viscous flow area, i.e. the core of the channel, and they are forced inwards again in the viscous boundary layer near the wall by the pressure gradient. So a helical secondary flow results.

Fig. 13 presents another typical phase distribution of the dispersed flow associated with intermediate or large mass flow rates and small to intermediate heat fluxes. Under these conditions film boiling is only partially maintained and rewetting can be found, firstly at the outer wall and later on spreading out to the inner wall after some axial distance.

In this figure the flow structure of the dispersed flow in the early stage of the bend looks similar to the case in fig.12. Beginning from about 45-deg. from the bend inlet a transition of local liquid distribution is observed. Liquid concentration is found both in the side region and in the inner region. However, the magnitude of the liquid concentration in the core remains small. This phenomenon

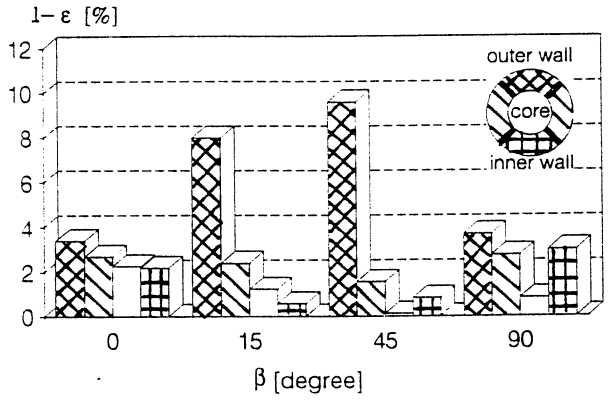

Figure 13: Phase distribution in bend with rewetting. (R_{bend}/R_{tube} = 42, Refrig. R12, p = 9,5 bar, $\dot{m}$ = 1240 kg/m^{2}s, $\dot{q}_W$ = 30 kW/m^2, $\dot{x}_{eq,in}$ = 0,81)

presents a question concerning the possible mechanism responsible for such rapid change of liquid concentration.

There could be the following explanation. It is to be expected that droplets having a diameter of more than 100 μm move either towards the symmetric plane or under the influence of the secondary flow towards the inner side along the circumference. As long as the wall is highly superheated, i.e. under film boiling conditions droplets may be fully evaporated on their way before they reach the inner side. This is obviously not true here. A realistic mechanism could be that under a sufficient deposition flux the hot wall is quenched to the temperature by which the droplets can impact and stay on the wall. These discrete droplets may form a continuous liquid film which flows towards the inner side of the bend under the action of the gravity and the interfacial shear stress.

To further study the nature of the dispersed flow structures effects of the mass flow rate the curvature ratio and the wall heat flux are discussed. A phase distribution factor F_j is introduced to describe the process of the phase separation and phase redistribution. It is defined as the ratio of liquid volume in the local region j to the total liquid volume measured in all five regions of the cross-section.

$$F_j = \frac{(1-\epsilon)_j \, A_j}{\sum_k (1-\epsilon)_k \, A_k} \qquad (26)$$

In equ.26 A_j represents the area of local region j. The factor F_j gives a relative magnitude of the local liquid fraction in the cross-section A_j compared to the total liquid fraction over all segments k. and by this provides a quantitative degree of the phase separation and redistribution. For heat transfer deliberations the behaviour of F_j in the outer an inner region is of main interest.

3.1 Effect of Mass Flow Rate.

Among the various influential parameters mass flow rate plays a key role to the dispersed flow structure. This is attributed to the fact that the magnitude of the mass flow rate influences strongly the mean velocity of the flow, the slip between the vapour and the entrained droplets and the droplet size. Usually larger mass flow rate corresponds to a higher bulk velocity and smaller droplets. As the centrifugal force is proportional to the square of the velocity an increase in velocity means a more significant centrifugal effect. Fig.14 shows liquid distributions at different mass flow rates.

It is clearly seen that with increasing mass flow rate more liquid droplets are centrifugally driven to the outside of the bend. Phase separation develops quite rapidly for all three flow rates within the first 15 deg. from the bend inlet. For the mass flow rate of 1240 kg/m^{2}s strong interaction of the droplets with the wall could significantly enhance the local heat transfer and result in a more accumulation of liqiuid droplets in the outer region. Different from this case for small mass flow the rapid change in liquid concentration between the outer and the inner region results in the formation of a liquid film over the circumference of the wall. For smaller mass flow rates the flow structure is dominated by the phase separation while the phase redistribution is less significant. This is due to the weaker secondary flow and a higher superheating of the vapour phase.

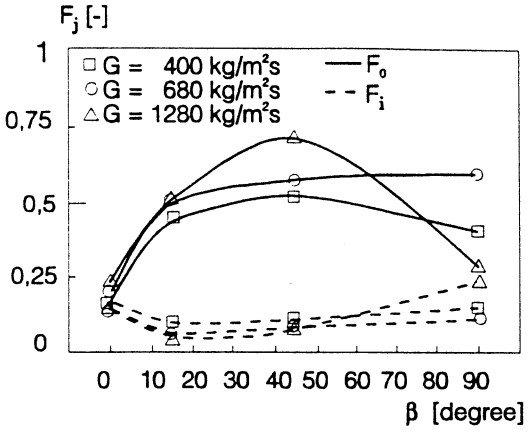

Figure 14: Effect of mass flow rate on phase distribution in a bend. (R_{bend}/R_{tube} = 42, Refrig. R12, p = 9,5 bar, $\dot{q}_W$ = 30 kW/m^2)

3.2 Effect of Curvature Ratio

In addition to mass flow rate the flow structure is also subjected to the influence of the curvature ratio or the bend radius. Fig.15 shows liquid distributions at two different bend radii with the same operational parameters.

A decrease of bend radius results in an increase in centrifugal acceleration and thus enforces the secondary flow. Increased centrifugal acceleration leads to a stronger phase separation in the early stage of the small radius bend. Once the liquid droplets enter into the wall region, however, they are subjected to the effect of the secondary

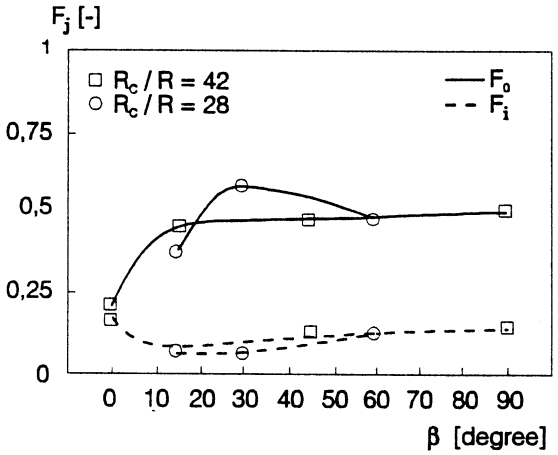

Figure 15: Effect of curvature ratio of the bend on phase distribution. (Refrig. R12, p = 9,5 bar, $\dot{m}$ = 680 kg/m^{2}s, $\dot{q}_W$ = 20 kW/m^2)

flow and are easier to be transported towards the inner side of the bend. As a result liquid inward circulation is much faster in the small radius bend than in the large radius one. Rapid change of the flow structure with a bend radius of 0,4m can, therefore, be observed in fig. 15.

3.3 The Effect of Heat Flux

Keeping all other parameters constant, wall heat flux considerably influences the flow structure only when it changes the heat transfer conditions on the heated wall, i.e. if film boiling is replaced by rewetting or if a wetted surface becomes dry. Fig. 16 presents profiles of liquid distribution in the outer and the inner region under different wall heat fluxes.

As can be seen from this figure, liquid distribution keeps nearly the same trend under wall heat fluxes ranging from 20 to 50 kW/m^2 where the rewetting statues maintains. In these cases a gradual transportation of the liquid from the outer to the inner region is observed as can be seen from the fact that the liquid concentration becomes smaller at the outer side of the bend and larger at the inner one. At a wall heat flux of 60 kW/m^2 the behaviour of the flow distribution in fig. 16 is different from the cases discussed before at the downstream end of the bend. The amount of heat removed by droplet impact is now no longer large enough to lower the wall temperature below the Leidenfrost point and to quench the wall. Under this wall conditions most droplets get evaporated either in the outer region of the cross section of the bend or on their way to the inner region. As a result the liquid concentration decreases only slightly in the outer region and does not show significant increase in the inner region.

In total the experiments showed an important change in the phase distribution along a bend compared to the case in straight channels. Strong interactions of the droplets with the vapour and the heated wall occur, which are initiated by the centrifugal force producing a phase separation. These features of the dispersed flow in bends are expected to have significant influence on the heat transfer performance.

4. CONCLUSIONS FOR SIZING

Fluiddynamic and thermodynamic disequilibria have a strong influence on the flow and on the heat transfer behaviour in boiling channels. At the entrance of a heat emitting channel with high heat flux densities subcooled boiling occurs already at a location where the bulk temperature is well below the saturation condition. The vapour formation reduces the free flow area for the liquid and produces additional momentum exchange and turbulence effects. All these phenomena result in an increased pressure loss. To calculate the pressure loss for designing the boiling channel, the development of the voidage has to be predicted by reliable physical models or

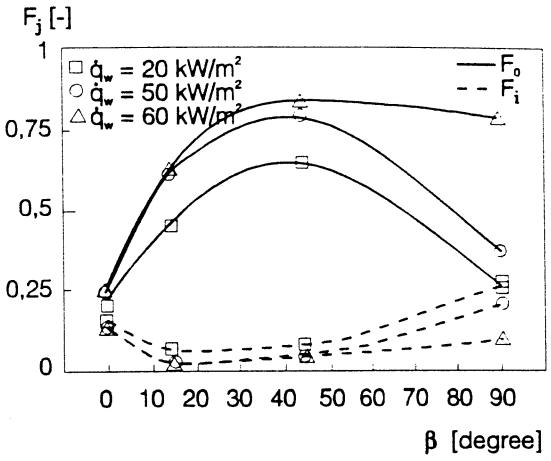

Figure 16: Effect of wall heat flux on the phase distribution in a bend. ($R_{bend}/R_{tube} = 42$, Refrig. R12, p=9,5 bar, $\dot{m} = 1240$ kg/m^{2}s)

empirical equations. A requirement for predicting the increase of the void fraction along the channel is a reliable knowledge about the point of onset of subcooled boiling and also about the recondensation of bubbles produced in the superheated boundary layer when coming in contact with the subcooled bulk flow. A too weak pumping power would have the consequences that the mass flow rate in the boiling channel does not reach its nominal value, which as a consequence produces more vapour and an earlier onset of subcooled boiling. The flow in the channel may become unstable and periodical flow oscillations may occur connected with varying heat transfer conditions and temperature oscillations of the wall or even a superheating of the wall beyond the design limits.

At the downstream end of the boiling channel spray cooling controls the wall temperature. There is a lot of information on spray cooling under post dry-out conditions in straight tubes. Very few was known up to now about the phase distribution in bends and its consequences on the heat transfer from the tube wall. Generally one can say that the average heat transport from the walls of a bend is better than that in a straight tube. However, locally large temperature differences can occur in bends due to phase separation resulting from the centrifugal force. Not always the heat transfer at the outer side of the bend is better than that of the inner side. Centrifugal forces move the droplets to the outer side, however. they also produce a pressure gradient from the outer to the inner side, which moves the liquid backwards to the inner side along the wall. So secondary flow in bends can promote rewetting and by this can remarkably improve the heat transfer.

REFERENCES

/1/ **Abdelmessih, A.H., Fakhri, A. & Yin, S.T.,** Proc. 5th Int. Heat Transfer Conference, Tokyo 4, (1974), pp. 165-169.

/2/ **Bjorge, R.W., Hall, G.R. & Rohsenow, W.M.,** Int. J. Heat Mass Transfer, 25 (1982) No.6, pp. 753-757.

/3/ **Bräuer, H., Mayinger, F.,** Subcooled Boiling Heat Transfer to R12 in an Annular Vertical Channel, In: Particulate Phenomena and Multiphase Transport, Ed.: T.N. Vezirogul - Washington: Hemisphere, Vol. 1, 1988, S. 443-458.

/4/ **Bräuer, H., Mayinger, F., Stängl, G.** Onset of Nucleate Boiling, Heat Transfer, Void Fraction and Pressure Drop in Subcooled Convective Boiling with R12, Proceedings of the 9th Int. Heat Transfer Conference, 1990, TPF 5, pp. 419-424.

/5/ **Bucher, B.,** Diss. Universität Hanover, 1979.

/6/ **Butterworth, D. & Shock, R.A.,** Proc. 7th Int. Heat Transfer Conference, Munich 1, (1982), pp. 11-30.

/7/ **Chen, Y.M.,** Wärmeübergang an der Phasengrenze kondensierender Blasen, Diss. Techn. Univ. München, 1985.

/8/ **Chen, Y.M., Mayinger, F.,** Measurement of Heat Transfer at the Phase Interface of Condensing Bubbles, Int. J. of Multiphase Flow, Vol. 18, No. 6, pp. 877-890, 1992.

/9/ **Dix, G.E.,** Vapour Void Fractions for Forced Convection with Subcooled Boiling at Low Flow Rates. Ph.D. Thesis, University of California, Berkerly, 1971.

/10/ **Dix, G.E.,** Ph.D. Thesis Univ. of California, 1970.

/11/ **Dougall, A.S. & Lippert, T.E.,** NASA Rep. , GR - 2241, 1973.

/12/ **Dougall, R.S. & Panian, D.J.,** NASA Contractor Report, GR - 2137, Washington, D.G., 1972.

/13/ **Friedel, L.,** Diss. Uni. Hannover, 1974.

/14/ **Hein, D. & Köhler, W.,** Report Nr. 43.02.05, MAN, 1968.

/15/ **Hein, D., Köhler, W., Mayinger, F.,** Chem.-Ing. Tech. 42, 1062 (1970).

/16/ **Macbeth, R.V. & Wood, R.W.,** European Two-Phase Flow Group Meeting, Univ. Strathclyde, 1980.

/17/ **Mayinger, F.,** Strömung und Wärmeübergang in Gas-Flüssigkeitsgemischen, Springer-Verlag, Wien, New York, 1982.

/18/ **Nordmann, D., Mayinger, F.,** Temperatur, Druck und Wärmetransport in der Umgebung kondensierender Blasen, VDI Forschungsheft Nr.: 605, S. 3 -36, 1981.

/19/ **Rouhani, S.Z.,** Calculation of Steam Volume Fraction in Subcooled Boiling. J. Heat Transfer 90, 158-164, 1968

/20/ **Saha, P., Zuber, N.,** Point of Net Vapour Generation and Vapour Void Fraction in Subcooled Boiling. Proceedings of the Int. Heat Transfer Conference Tokyo, Vol. 4, Paper B 4.7, 1974.

/21/ **Spindler, K. & Hahne, E.,** Chem.-Ing.-Technik, Bd. 60, Nr. 1, (1988), pp. 54-55.

/22/ **Stängl, G., Mayinger, F.,** Void Fraction and Pressure Drop in Subcooled Forced Convective Boiling with Refrigerant R12, Proceedings of the Int. Conf. on Mechanics of Two-Phase Flow, Taiwan, 1989, E.d.R.S.L. Lee and F. Durst, Taiwan University.

/23/ **Staub, F.W.,** The Void Fraction in Subcooled Boiling Prediction of the Initial Point of Net Vapour Generation, ASME 67 - HT - 36, Aug. 1967.

/24/ **Staub, F.W., Walmet, G.E. & Niemi, R.O.,** Final Report NYO-3679-8, 1969.

/25/ **Wang, M.Y.,** Phasenverteilung, Sekundärströmung und Wärmeübergang bei Sprühkühlung in Krümmern. Diss. Techn. Univ. München, 1993.

/26/ **Wang, M., Mayinger, F.,** Droplet Distribution and Heat Transfer of Post-dryout Dispersed Flow in 90-deg. Circular Bends. ANS Proc. of the Nat. Heat Transfer Conf., Minneapolis, Minnesota, July 28-31, 1991. Minneapolis: Americ. Nucl. Soc. 1991, Vol. 5, S. 75-82.

/27/ **Zuber, N. & Findlay, J.A.,** J. of Heat Transfer, 87, 1965.